Liquid Crystals
Publication details, including instructions for authors and subscription information:
http://www.informaworld.com/smpp/title~content=t713926090

Synergisms, structure-material relations and display performance of novel fluorinated alkenyl liquid crystals

Martin Schadt[a]; Richard Buchecker[a]; Alois Villiger[a]
[a] Central Research Units, F. Hoffmann-La Roche Ltd, Basel, Switzerland

To cite this Article Schadt, Martin , Buchecker, Richard and Villiger, Alois(1990) 'Synergisms, structure-material relations and display performance of novel fluorinated alkenyl liquid crystals', Liquid Crystals, 7: 4, 519 — 536
To link to this Article: DOI: 10.1080/02678299008033829
URL: http://dx.doi.org/10.1080/02678299008033829

LIQUID CRYSTALS, 1990, VOL. 7, NO. 4, 519-536

Synergisms, structure-material relations and display performance of novel fluorinated alkenyl liquid crystals

by MARTIN SCHADT, RICHARD BUCHECKER and ALOIS VILLIGER
Central Research Units, F. Hoffmann-La Roche Ltd, CH-4002 Basel, Switzerland

(*Received 14 September 1989; accepted 10 November 1989*)

Several new classes of low polarity, low viscosity and optically weakly anisotropic two and three ring fluorinated liquid crystals with alkenyl side chains are presented. Synergisms which lead to a number of favourable material properties are shown to result from systematic changes of (*a*) para and lateral fluorination of the benzene ring in the rigid cores, (*b*) variations of double bond positions in the alkenyl side chains and (*c*) from replacing cyclohexane core rings by dioxane rings. A broad range of dielectric anisotropies $-0.3 < \Delta\varepsilon < 13$, broad nematic mesophases, low rotational, γ_1 and bulk viscosities, η, (22°C) < 10 cP as well as visco elastic ratios as low as γ_1/κ (22°C) $= 3{\cdot}8 \times 10^{-12}\,\mathrm{m}^{-2}\,\mathrm{s}^{-1}$ follow; were $\kappa = k_{11} + (k_{33} - 2k_{22})/4$. As a consequence a wide range of optical threshold voltages V_{10} and short response times result in field-effect liquid crystal displays. The low ratios $\kappa/\Delta\varepsilon$ of the heterocyclic representatives among the new compounds lead in twisted nematic displays to threshold voltages which are comparably as low as those of (polar) phenylcyclohexane compounds. In agreement with our earlier results pronounced odd-even effects are shown to result from shifting the aklenyl double bond in the new compounds from even to odd side chain sites. This causes $\Delta\varepsilon$ to increase by 40 per cent and γ_1 by 33 per cent. Both odd-even effects are shown to be due qualitatively to the increase of side chain order parameter which is expected from shifting the alkenyl double bond from even into odd sites.

1. Introduction

A prerequisite for the operability of all liquid crystal displays based on electron-optic field effects are liquid crystals exhibiting a dielectric anisotropy $\Delta\varepsilon = (\varepsilon_{\parallel} - \varepsilon_{\perp}) \neq 0$. Thus, twisted nematic displays and supertwisted nematic displays require positive dielectric anisotropic materials ($\Delta\varepsilon > 0$); whereas positive contrast guest-host displays and electric field controlled birefringence displays often require materials with $\Delta\varepsilon < 0$ [1]. With increasing dielectric anisotropy, $|\Delta\varepsilon|$, the threshold voltage of the displays decrease. Unfortunately, this desirable behaviour is accompanied by an increase of liquid crystal viscosity which causes the response times of the display to increase too. This is due to dipole–dipole interactions of the strongly polar terminal groups which induce a dimer-like association of molecules thus increasing the inertia of rotation around the short molecular axes [2].

Apart from their larger viscosity, liquid crystals with $\Delta\varepsilon \gg 0$ exhibit a strongly enhanced solubility for ionic impurities. Therefore, polar compounds tend to dissolve residual ionic impurities from the adjacent polymer wall aligning layers of liquid crystal displays much more effectively than less polar compounds. As a consequence there is a reduction of the initially large specific resistivity of the liquid crystal layer and an increase of the display current. Whereas reasonably small current increases do not affect the operability of time multiplexed displays, this no longer holds when driving liquid crystal displays via an active substrate, such as with integrated thin film

0267-8292/90 $3.00 © 1990 Taylor & Francis Ltd

transistors [3]. In this case, increasing the residual ohmic current across the (storage) capacitance of each picture element shortens the storage time of the pixels and therefore leads, especially at elevated temperatures, to a reduction of the multiplexibility of such displays. Thus, fast responding liquid crytals are required which lead to still rather low threshold voltages without exhibiting excessively large polarities.

Here we introduce a number of new, non-polar ($\Delta\varepsilon \sim 0$) as well as weakly polar ($\Delta\varepsilon > 0$) nematic liquid crystals with aklenyl side chains. The compounds belong to different structural classes. Their common features are low viscosities as well as low optical anisotropies. The three ring as well as some two ring compounds exhibit broad nematic mesophases which lead to fast responding mixtures with high nematic-isotropic transition temperatures. The new compounds differ from each other with respect to (*a*) the systematic changes made in the position of the alkenyl double bond in their side chains, (*b*) their rigid cores which also comprise heterocyclic rings, (*c*) the introduction of fluoro substituents at different positions in the phenyl ring of their rigid cores and (*d*) the combination of alkenyl side chains with alkyl and alkylmethyleneoxy side chains. The elastic, dielectric, optical and viscous properties of the new liquid crystals are shown to extend further the broad range of material properties of low birefringence nematics [4]. Moreover, correlations between different molecular structural elements and material properties are shown.

2. New alkenyl liquid crystals

2.1. *Two ring alkenyls*

The low viscous, non-polar phenylcyclohexane 3CPO$d_3$1 [5] at the top of table 1 serves as a reference compound, it is used as one of the two components in all binary mixtures to lower (*a*) the mesomorphic range of mixtures comprising three ring components, thus allowing viscosity and electro-optic measurements to be made down to room temperature; (*b*) to increase the diamagnetic anisotropy of the samples to be investigated such that most of them can be aligned in magnetic fields; and (*c*) to investigate the changes of material properties when combining components with different polarity and different molar proportions. The two polar cyano nematics 1d_1CC and 1d_1CP [4, 5] are also used as reference compounds. The nomenclature used here is analogous to that described earlier [4]: alkenyl double bond is d_x, where the index designates the position of the bond from the nearest core ring, that is from the cyclohexane ring C, the phenyl ring P or the dioxane ring D. The numbers in front of d_x are those of the carbon atoms attached to d_x.

The only LCs which exhibit partial smectic B phases in table 1 are the non-polar alkenyl-alkylmethyleneoxy 1d_1CC1O1 and the alkenyl-alkyl 0d_1CC5 both of which possess unusually broad mesomorphic ranges. However, because there are in both cases broad nematic phases superimposed (see table 1), their S_B tendencies are completely suppressed in mixtures. Thus, the nematic mixtures M1–M3 exhibit low melting and high clearing temperatures. (see table 1).

The two weakly polar, para fluorinated 0d_3-alkenyls 0d_3CPF and 0d_3DPF are pronouncedly monotropic. Therefore, they induce large depressions of the transition temperatures in M4 and M5 (see table 1). It is interesting to note in table 1 that the (extrapolated) dielectric anisotropy $\Delta\varepsilon^*$ (0d_3DPF) is about three times as large as $\Delta\varepsilon^*$ (0d_3CPF) and comparable to $\Delta\varepsilon$ (1d_1CC). Moreover, it follows from the data in table 1 that the combination of a terminal cyano group and a benzene ring in 1d_1CP

Table 1. Single components and binary mixtures M1–M7 of two ring alkenyl liquid crystals comprising bicyclohexanes (CC), dioxane rings (D) and para fluorinated phenyl rings (P). The non-polar, low viscous phenylcyclohexane nematic 3CPO$d_3$1, as well as the polar cyano-phenylcyclohexane 1d_1CP and the cyano-bicyclohexane 1d_1CC serve as reference compounds [4, 5]. T_m, melting temperature; T_{NI}, nematic-isotropic transition; $\Delta\varepsilon$, dielectric anisotropy determined in the respective single components at (T_{NI} − 10°C); $\Delta\varepsilon^*$, dielectric anisotropy of the single component extrapolated from the binary mixture data.

Nomenclature	Structure	T_m/°C	T_{SN}/°C	T_{NI}/°C	$\Delta\varepsilon$ (T_{NI} − 10°C)
3CPO$d_3$1	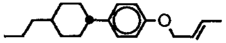	42·4		57·5	−0·27
1d_1CC1O1	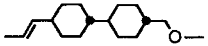	12·3	22·4	62·2	−0·17
d_1CC5	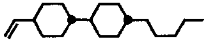	−8	52	63·4	0·7
0d_3CPF	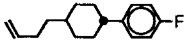	31·3		−36	1·6*
d_3DPF	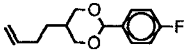	46·3		−45	4·6*
1d_1CC	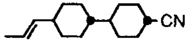	64·9		99·7	5·0
1d_1CP	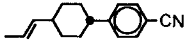	66·5		73·0	15·2
M1 = (**1d_1CC1O1**, 3CPO$d_3$1)	(20 : 80 mol %)	27		54·8	
M2 = (**1d_1CC1O1**, 3CPO$d_3$1)	(50 : 50 mol%)	< 15		52·3	
M3 = (**0d_1CC5**, 3CPO$d_3$1)	(50 : 50 mol %)	< 15		54·1	
M4 = (**0d_3CPF**, 3CPO$d_3$1)	(20 : 80 mol %)	24		43·2	
M5 = (**0d_3DPF**, 3CPO$d_3$1)	(20 : 80 mol %)	22		41·2	
M6 = (**1d_1CC**, 3CPO$d_3$1)	(20 : 80 mol %)	27		55·3	
M7 = (**1d_1CP**, 3CPO$d_3$1)	(20 : 80 mol %)	25		55·9	

increases the dielectric anisotropy by a factor of three compared with $\Delta\varepsilon$ ($1d_1$CC). This shows that it is not the cyano group per se which leads to large dielectric anisotropies for liquid crystals but only its conjugation with an aromatic ring.

2.2. *Three ring alkenyls*

Table 2 shows (at the top) the three ring alkenyl-alkyl compounds $1d_1$CCP1 and $0d_3$CCP1 as well as a series of five new para fluorinated three ring alkenyls with double bonds at different chain positions. From the two pairs of compounds with identical side chains, namely $0d_1$ and $0d_3$, follows the influence of the replacement of the methyl group by a fluorine atom in $1d_1$CCP1 and $0d_3$CCP1, which leads to $1d_1$CCPF and $0d_3$CCPF. The systematic shift of the double bonds in the side chains of the fluorinated alkenyls listed in table 2 were made to investigate the dependence of the material parameters of para fluorinated alkenyls on the double bond position. Due to the limited solubility of three ring components, molar proportions of 20 : 80 were chosen for all of the mixtures.

From the data in table 2 follows that replacing CH_3 by F in $0d_3$CCP1, which leads to $0d_3$CCPF, suppresses the S_B phase of $0d_3$CCP1 completely and increases the dielectric anisotropy by a factor of six. In agreement with our earlier findings [4] in cyano alkenyls, the largest dielectric anisotropies results for the odd double bond positions $1d_1$ and $1d_3$ (see table 2). Also in line with our earlier results are the depressions of the transition temperatures for even positions (see $0d_4$ in table 2), whereas a strong increase of the transition occurs for odd positions [4, 5]; c.f. $1d_1$ and $1d_3$ in table 2. Contrary to our earlier results which showed that even double bond positions strongly favour the occurrence of S_B phases in cyano as well as in alkyl-alkenyls, this does not hold in para fluorinated alkenyls; c.f. $0d_4$CCPF in table 2. As a consequence of para fluorination all of the F-alkenyls in table 2 are purely nematic.

Table 3 shows new, laterally fluorinated three ring $1d_1$-alkenyls, including rigid cores which comprise one dioxane ring. Besides from the directly linked ring systems, table 3 also lists the ester-linked compound $1d_1$CCEPF for comparison of mesophases. To compare the effects of para, lateral and difluoro substitution of the aromatic ring in $1d_1$-alkenyls, $1d_1$CCP1 and $1d_1$CCPF (see table 2) are included in table 3. From the dielectric anisotropies of the single components in table 3 we find the order

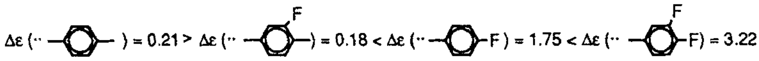

of dielectric anisotropy at the respective temperature (T_{NI} − 10°C). Thus, para fluorination increases the dielectric anisotropy by a factor of eight ($1.75/0.21 \approx 8$), whereas the combination of para and lateral fluorination adds another factor of two ($3.22/1{,}75 \approx 2$). Moreover, from $\Delta\varepsilon(1d_1\mathrm{CCPF}) = 1{\cdot}75 < \Delta\varepsilon(1d_1\mathrm{DCPF}) = 6{\cdot}8$ and $\Delta\varepsilon(1d_1\mathrm{CCPF_F F}) = 3{\cdot}22 < \Delta\varepsilon(1d_1\mathrm{DCP_F F}) = 12{\cdot}4$ given in table 3 it follows that the replacement in the rigid cores of one cyclohexane ring C by the optically comparably isotropic dioxane ring D scales the dielectic anisotropies and increases $\Delta\varepsilon$ by another factor of four. Thus, the rather small oxygen permanent dipole moments of the dioxane ring D considerably extend the range of $\Delta\varepsilon$ of optically weakly anisotropic fluorinated compounds. From these results it follows that this can be achieved without the use of strong permanent dipole moments in conjugation with aromatic rings as in $1d_1$CP (see table 1).

Table 2. Single, three ring alkenyl components with either alkyl side chains or para fluoro substituents and binary mixtures M8–M14. Except for 0d_3CCP1, which exhibits an S_B phase, all components and mixtures are nematic.

Nomenclature	Structure	T_m/°C	T_{SN}/°C	T_{NI}/°C	Δε (T_{NI} − 10°C)
1d_1CCP1	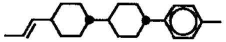	74		214	0·21
0d_3CCP1	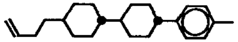	52	104	177	0·19
0d_1CCPF	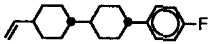	85		145	1·35
1d_1CCPF	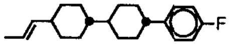	105		194	1·75
0d_3CCPF	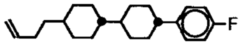	82		157	1·25
1d_3CCPF	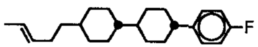	83		175	1·65
0d_4CCPF	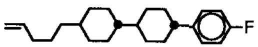	66		130	1·19
M8 = (**1d_1CCP1**, 3CPO$d_3$1)	(20 : 80 mol %)	22		78·1	
M9 = (**0d_3CCP1**, 3CPO$d_3$1)	(20 : 80 mol%)	30		76·1	
M10 = (**0d_1CCPF**, 3CPO$d_3$1)	(20 : 80 mol %)	22		68·0	
M11 = (**1d_1CCPF**, 3CPO$d_3$1)	(20 : 80 mol %)	32		75·0	
M12 = (**0d_3CCPF**, 3CPO$d_3$1)	(20 : 80 mol %)	25		72·5	
M13 = (**1d_3CCPF**, 3CPO$d_3$1)	(20 : 80 mol %)	22		77·7	
M14 = (**0d_4CCPF**, 3CPO$d_3$1)	(20 : 80 mol %)	22		69·5	

Table 3. Single, three ring alkenyl components with identical 1d_1-alkenyl side-chains, different fluoro substituents and/or dioxane rigid cores, as well as binary mixtures M15–M19. Note that M19 comprises 0d_1CCEPF and not 1d_1CCEPF.

Nomenclature	Structure	T_m/°C	T_{SN}/°C	T_{NI}/°C	Δε (T_{NI} − 10°C)
1d_1CCP1	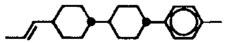	74		214	0·21
1d_1CCP$_F$1	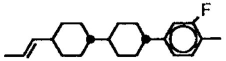	87		186	0·18
1d_1CCPF	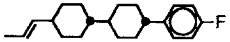	105		194	1·76
1d_1CCP$_F$F	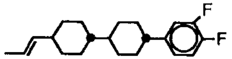	49	65	159	3·22
1d_1DCPF	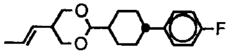	111		160	6·80
1d_1DCP$_F$F	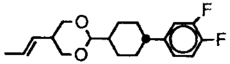	96		125	12·4
1d_1CCEPF		75		209	
M15 = (**1d_1CCP$_F$1**, 3CPO$d_3$1)	(20 : 80 mol %)	26		71·7	
M16 = (**1d_1CCP$_F$F**, 3CPO$d_3$1)	(20 : 80 mol%)	25		68·9	
M17 = (**1d_1DCPF**, 3CPO$d_3$1)	(20 : 80 mol %)	25		67·2	
M18 = (**1d_1DCP$_F$F**, 3CPO$d_3$1)	(20 : 80 mol %)	22		60·9	
M19 = (**0d_1CCEPF**, 3CPO$d_3$1)	(20 : 80 mol %)	20		74·1	

It came as a surprise to us to see that lateral fluorination leads for 1d_1CCP$_F$1 to a very small dielectric anisotropy $\Delta\varepsilon$ (1d_1CCP$_F$1) = 0·18, whereas the same structural change synergetically increases $\Delta\varepsilon$ strongly if combined with para fluorination:$\Delta\varepsilon$ (1d_1CCPF) = 1·75 → $\Delta\varepsilon$ (1d_1CCP$_F$F) = 3·22 (see table 3). This apparent discrepancy seems to be due to a partial compensation of the lateral C–F permanent dipole moment by an oppositely directed dipole moment which originates from the formation of a hydrogen bridge with the protons of the methyl group in 1d_1CCP$_F$1:

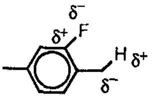

Since no hydrogen bridges can occur in 1d_1CCPF or 1d_1CCP$_F$F the associated dielectric anisotropies are larger (see table 3).

It is interesting to note in table 3 that neither 1d_1CCP$_F$1 nor 1d_1CCPF exhibit smectic phases. However, a S$_B$ phase occurs when combining lateral and para-fluorination; cf. 1d_1CCP$_F$. This indicates that fluoro substitution does not per se improve nematic behaviour.

3. Material properties

3.1. *Dielectric, elastic and optical constants*

Table 4 lists the elastic, dielectric (static) and optical properties of the reference compound 3CPO$d_3$1 and of mixtures M1–M7 which comprise the two ring alkenyls depicted in table 1. As summary of the measuring techniques and the problems involved in investigating liquid crystals with virtually isotropic diamagnetic susceptibilities is given in [4]. The data in bold type were determined at the temperatures (T_{NI} − 10°C) which follow from table 1, the others are room temperature data (22°C). In those cases where the melting temperatures of mixtures M1–M19 are above 22°C, extrapolated values are used which follow from the temperature dependence of the respective material parameters. Because the temperature dependence of the material parameters in table 2 scales with the nematic order parameter $S(T)$ [6], comparisons among different compounds should be made at (T_{NI} − 10°C).

From the decrease of the splay (k_{11}) elastic constant and from the slight increase of the bend/splay elastic ratio k_{33}/k_{11} in M1 and M2 shown in table 4 it follows that k_{11} and k_{33} of the broad range alkenyl-alkylmethyleneoxy compound 1d_1CC1O1 are considerably smaller than those of the reference 3CPO$d_3$1. The same holds for the elastic constant expression

$$\kappa = [k_{11} + (k_{33} - 2k_{22})/4]$$

whose decrease causes a reduction of the optical threshold voltage in twisted nematic displays [4]. The comparably small changes of the elastic and dielectric constants between M1 and M2, compared with those between M1 and 3CPO$d_3$1 (see table 4), indicate that care has to be taken when determining the material parameters of a single component from a linear extrapolation of mixture data. On the other hand, the rather small changes among k_{ii} and $\Delta\varepsilon$ between M1 and M2 shows that the molar proportions 20 : 80 used in the mixtures are sufficient to indicate at least the trend towards which k_{ii}, Δn and $\Delta\varepsilon$ of the single component tend. Because of the 50 : 50 molar proportions of M2 and M3, their data can be compared directly with those of the bicyclohexane alkenyls recently published [4].

Table 4. Splay (k_{11}), twist (k_{22}) and bend/splay (k_{33}/k_{11}) elastic constants; elastic expression $\kappa = k_{11} + (k_{33} - 2k_{22})/4$; dielectric anisotropy $\Delta\varepsilon = (\varepsilon_{\parallel} - \varepsilon_{\perp})$ and optical anisotropy $\Delta n = (n_e - n_o)$ of the reference compound 3CPO$d_3$1 and of the binary mixtures M1–M7 of table 1. The data in bold type were determined at (T_{NI} − 10°C), whereas the others are room temperature data (23°C).

Liquid crystal	$k_{11}/10^{-12}$ N	$k_{22}/10^{-12}$ N	k_{33}/k_{11}	$\kappa/10^{-12}$ N	$\varepsilon_{\perp}$	$\Delta\varepsilon$	n_o	Δn
3CPO$d_3$1 (100 per cent)	**8·82**	**4·55**	**1·16**	**9·1**	**3·07**	**−0·268**	**1·486**	**0·089**
M1 = (**1d_1CC1O1**, 3CPO$d_3$1)	**8·12**	**4·25**	**1·26**	**8·5**	**3·10**	**−0·262**	**1·483**	**0·083**
20 80	13·8	6·63	1·34	15·1	3·22	−0·360	1·488	0·100
M2 = (**1d_1CC1O1**, 3CPO$d_3$1)	**7·84**	**4·34**	**1·22**	**8·1**	**3·07**	**−0·241**	**1·478**	**0·071**
50 50	12·6	6·20	1·29	13·6	3·19	−0·330	1·482	0·085
M3 = (**0d_1CC5**, 3CPO$d_3$1)	**6·67**	**3·49**	**1·08**	**6·7**	**2·62**	**−0·011**	**1·477**	**0·062**
50 50	11·5	5·70	1·06	11·7	2·68	−0·033	1·482	0·076
M4 = (**0d_3CPF**, 3CPO$d_3$1)	**7·00**	**3·60**	**1·17**	**7·3**	**3·16**	**0·100**	**1·491**	**0·084**
20 80	10·2	4·50	1·19	11·0	3·18	0·120	1·493	0·096
M5 = (**0d_3DPF**, 3CPO$d_3$1)	**8·17**	**4·08**	**1·11**	**8·4**	**3·69**	**0·705**	**1·491**	**0·086**
20 80	10·9	5·10	1·13	11·5	3·71	0·820	1·492	0·096
M6 = (**1d_1CC**, 3CPO$d_3$1)	**7·81**	**4·33**	**1·28**	**8·2**	**3·50**	**1·36**	**1·485**	**0·084**
20 80	12·9	6·39	1·39	14·2	3·52	1·70	1·489	0·102
M7 = (**1d_1CP**, 3CPO$d_3$1)	**8·22**	**4·18**	**1·32**	**8·8**	**3·73**	**2·77**	**1·489**	**0·096**
20 80	13·8	6·36	1·38	15·4	3·68	3·54	1·493	0·117

Table 5. Elastic, dielectric and optic material constants of binary mixtures M8–M14 of table 2. The data in bold type were determined at (T_{NI} − 10°C), whereas the others are 22°C data.

Liquid crystal	$k_{11}/10^{-12}$ N	$k_{22}/10^{-12}$ N	k_{33}/k_{11}	$\kappa/10^{-12}$ N	$\varepsilon_\perp$	$\Delta\varepsilon$	n_o	Δn
M8 = (**1d_1CCP1**, 3CPO$d_3$1)	**7·76**	**4·14**	**1·23**	**8·1**	**2·81**	**−0·110**	**1·484**	**0·085**
	17·5	7·37	1·39	20·0	2·98	−0·220	1·493	0·114
M9 = (**0d_3CCP1**, 3CPO$d_3$1)	**7·31**	**4·00**	**1·14**	**7·4**	**2·83**	**−0·113**	**1·484**	**0·079**
	17·1	7·60	1·22	18·5	2·95	−0·220	1·494	0·109
M10 = (**0d_1CCPF**, 3CPO$d_3$1)	**8·05**	**4·08**	**1·16**	**8·3**	**3·02**	**0·181**	**1·485**	**0·081**
	16·0	6·92	1·19	17·3	3·38	0·222	1·493	0·105
M11 = (**1d_1CCPF**, 3CPO$d_3$1)	**8·31**	**4·10**	**1·22**	**8·8**	**2·99**	**0·359**	**1·482**	**0·083**
	17·9	7·15	1·31	20·2	3·14	0·485	1·498	0·111
M12 = (**0d_3CCPF**, 3CPO$d_3$1)	**7·77**	**4·18**	**1·16**	**7·9**	**2·94**	**0·213**	**1·484**	**0·079**
	16·9	7·15	1·21	18·4	3·08	0·266	1·493	0·105
M13 = (**1d_3CCPF**, 3CPO$d_3$1)	**7·74**	**3·82**	**1·25**	**8·2**	**2·95**	**0·353**	**1·482**	**0·080**
	17·7	7·30	1·35	20·0	3·11	0·483	1·493	0·109
M14 = (**0d_4CCPF**, 3CPO$d_3$1)	**7·24**	**3·71**	**1·10**	**7·4**	**2·97**	**0·219**	**1·485**	**0·077**
	15·9	6·51	1·10	16·9	3·11	0·284	1·492	0·103

From the results for M3 in table 4 it follows that k_{33}/k_{11} and κ for the bicyclohexane alkyl-alkenyl 0d_1CC5 are lower than those of 3CPO$d_3$1 or 1d_1CC1O1, its optical anisotropy is also lower. Because of the lack of the oxygen dipole moment the (small) dielectric anisotropy of 0d_1CC5 changes sign (see table 1). The low elastic constant ratio k_{33}/k_{11} for 0d_1CC5 leads to an increase of the steepness of the transmission-voltage characteristics of twisted nematic displays, whereas its low κ-value, combined with its slightly positive dielectric anisotropy, contribute to lowering the threshold voltage of mixtures designed for twisted nematic displays operated in the first transmission minimum [1, 4].

Comparing the data of M4 and M5 which comprises para fluorinated alkenyls with those of M1–M3 as well as with M6 and M7 in table 4 shows (*a*) rather low elastic constant ratios, k_{33}/k_{11}, especially for M5 (*b*) a pronounced increase of $\Delta\varepsilon$ in M5 compared with $\Delta\varepsilon$ (M4) and (*c*) optical anisotropies, Δn, which are comparable to those of 3CPO$d_3$1. Whereas the low elastic constant ratio k_{33}/k_{11} (M5) can be attributed to the heterocyclic dioxane ring D [1] in 0d_3DPF, the strong, two step increase of the dielectric anisotropy from $\Delta\varepsilon$ (3CPO$d_3$1) $= -0{\cdot}27 \rightarrow \Delta\varepsilon$ (M4) $= 0{\cdot}10 \rightarrow \Delta\varepsilon$ (M5) $= 0{\cdot}70$ is a consequence of (i) para fluorination and (ii) the synergism resulting from para fluorination and the introduction of the dioxane ring D in 0d_3DPF.

Table 5 shows the elastic, dielectric and optical properties of mixtures M8, M9 and their para fluorinated counterparts M11 and M12. M10–M14 comprise the para fluorinated alkenyls with different double bond positions (cf. also table 2). From the data for M8, M9, M11 and M12 it follows that the elastic and optical properties do hardly change upon replacing CH_3 in Yd_xCCP1 by a fluorine atom. However, para fluorination causes the dielectric anisotropy to change sign and to increase strongly. From the elastic constants for M13 and M14 it follows that even double bond positions in para fluorinated alkenyls decrease k_{33}/k_{11} as well as κ. This finding, though less pronounced, is in agreement with our earlier results in cyano alkenyls [5] and bicyclohexane alkenyls [4].

Changing the position of the double bond from an even (0d_4) into an odd position (1d_3), while keeping the length of the alkenyl side chains constant, does not only affect the elastic constants but also increases the optical and especially the dielectric anisotropy; cf. M13, M14 in table 5. The increase of $\Delta\varepsilon$ in M13 by 60 per cent compared with $\Delta\varepsilon$ (M14) is remarkably larger and much more pronounced than in the dielectrically stronger anisotropic cyano alkenyls [5]. This is due to the generally lower $\Delta\varepsilon$ level of the fluorinated alkenyls shown in table 5 compared with the strongly polar cyano-phenylcyclohexane alkenyls (cf. M7 in table 4 and [5]). As a consequence, variations of chain length and/or double bond position which affect the induced dipole moments influence $\Delta\varepsilon$ of the fluorinated alkenyls more strongly. This can be seen from $\Delta\varepsilon$ for M12, M13 compared with M10, M11 in table 5. The dielectric odd–even effect (see table 5) is due to positional dependent alignment of the π-electron –C=C– double bonds whose average projection parallel to the molecular long axis in odd positions is larger than in even positions [5, 7]. Therefore, and because of the considerably larger molecular order parameter for the terminal C–H segment of 1d_1- and 1d_3-double bond positions, which follows from NMR investigations [8], the corresponding induced dipole moments parallel to **n** increase, thus increasing $\Delta\varepsilon$ too.

Except for M19 all mixtures in table 6 comprise alkenyls with identical (1d_1) side chains (cf. also table 3). Table 6 shows the effects of para and lateral fluorination as well as the effect of replacing one cyclohexane ring C by the dioxane ring D on the

Table 6. Elastic, dielectric and optic material constants of binary mixtures M15–M19 comprising the para and laterally fluorinated alkenyls of table 3. The data in bold type were determined at (T_{NI} − 10°C), whereas the others are 22°C data.

Liquid crystal	$k_{11}/10^{-12}$ N	$k_{22}/10^{-12}$ N	k_{33}/k_{11}	$\kappa/10^{-12}$ N	$\varepsilon_\perp$	$\Delta\varepsilon$	n_o	Δn
M8 = (**1d_1CCP1**, 3CPO$d_3$1)	**7·76**	**4·14**	**1·23**	**8·1**	**2·81**	**−0·110**	**1·484**	**0·085**
	17·5	7·37	1·39	20·0	2·98	−0·220	1·493	0·114
M15 = (**1d_1CCP$_F$1**, 3CPO$d_3$1)	**8·11**	**4·10**	**1·18**	**8·5**	**3·02**	**−0·150**	**1·483**	**0·087**
	17·0	7·15	1·27	18·8	3·20	−0·262	1·492	0·112
M11 = (**1d_1CCPF**, 3CPO$d_3$1)	**8·31**	**4·10**	**1·22**	**8·8**	**2·99**	**0·359**	**1·482**	**0·083**
	17·9	7·15	1·31	20·2	3·14	0·485	1·498	0·111
M16 = (**1d_1CCP$_F$F**, 3CPO$d_3$1)	**7·86**	**4·03**	**1·16**	**8·10**	**3·24**	**0·687**	**1·482**	**0·084**
	16·7	6·56	1·20	18·4	3·39	0·971	1·491	0·109
M17 = (**1d_1DCPF**, 3CPO$d_3$1)	**7·89**	**4·14**	**1·30**	**8·4**	**3·46**	**1·544**	**1·484**	**0·086**
	14·9	6·97	1·42	16·7	3·56	2·100	1·491	0·110
M18 = (**1d_1DCP$_F$F**, 3CPO$d_3$1)	**8·28**	**4·22**	**1·21**	**8·7**	**3·83**	**2·378**	**1·484**	**0·085**
	15·2	7·24	1·25	16·3	3·89	3·314	1·490	0·107
M19 = (**0d_1CCEPF**, 3CPO$d_3$1)	**7·86**	**4·15**	**1·17**	**8·1**	**3·21**	**0·202**	**1·482**	**0·077**
	17·2	7·71	1·20	18·5	3·42	0·230	1·490	0·104

Table 7. Bulk (η) and rotational (γ_1) viscosities; viscoelastic ratio γ_1/κ; dielectric anisotropy $\Delta\varepsilon$; V_{10}, threshold voltage of a twisted nematic display with $d = 6\,\mu$m cell gap at 10 per cent transmission; t_{on}, turn-on time of the display for 0 per cent to 90 per cent transmission; t_{off}, turn-off time of the display for 100 per cent to 10 per cent transmission of mixtures M1–M7 (table 1). The data in bold type were determined at (T_{NI} − 10°C), whereas the others are 22°C data.

Liquid crystal	η/cP	γ_1/cP	$\gamma_1^{-1}\kappa/10^{-12}$ m^{-2} s^{-1}	$\Delta\varepsilon$	V_{10}/V	t_{on}/ms	t_{off}/ms
3CPO$d_3$1 (100 per cent)	**4·7**	**25**	**2·7**	**−0·268**	–	–	–
	13·5	86					
M1 = (**1d_1CC1O1**, 3CPO$d_3$1)	**5·9**	**21·7**	**2·5**	**−0·262**	–	–	–
20 80	11·5	60	4·0	−0·360			
M2 = (**1d_1CC1O1**, 3CPO$d_3$1)	**6·1**	**20·6**	**2·5**	**−0·241**	–	–	–
50 50	10·8	51·4	3·8	−0·330			
M3 = (**0d_1CC5**, 3CPO$d_3$1)	**5·2**	–	–	**−0·011**	–	–	–
50 50	9·6	–	–	−0·033			
M4 = (**0d_3CPF**, 3CPO$d_3$1)	**7·1**	–	–	**0·100**	**9·5**	**8·3**	**12·3**
20 80	9·8	–	–	0·120	10·8	10	14
M5 = (**0d_3DPF**, 3CPO$d_3$1)	**8·4**	**32·5**	**3·9**	**0·705**	**3·9**	**7·6**	**14·2**
20 80	10·5	60	5·2	0·820	4·3	9·0	16
M6 = (**1d_1CC**, 3CPO$d_3$1)	**6·8**	**24·9**	**3·0**	**1·36**	**2·8**	**5·6**	**11·0**
20 80	14·3	105	7·4	1·70	3·5	13	17
M7 = (**1d_1CP**, 3CPO$d_3$1)	**5·8**	**23·9**	**2·7**	**2·77**	**2·1**	**5·3**	**9·2**
20 80	13·3	82	5·3	3·54	2·8	7·4	14

elastic, dielectric and optic properties of $1d_1$-alkenyls. Mixture M8 serves as a non-fluorinated reference. From the similar elastic and optical properties of the mixtures in table 6 it follows that the structural changes among the compounds in table 6 do not affect significantly k_{ii}, k_{33}/k_{11}, κ or Δn. However, the dielectric data in table 6 shows a strong influence of the molecular structural changes on the dielectric anisotropy. These are most obvious when comparing the dielectric anisotropies of the single components in table 3. It follows that $\Delta\varepsilon$ can be increased step wise by either lateral, para or lateral + para fluorination and/or by replacement of a cyclohexane ring C by a dioxane ring D. The synergetic effects which result from combining $\Delta\varepsilon$ (D) + $\Delta\varepsilon$ (difluoro) lead to $\Delta\varepsilon$ ($1d_1\mathrm{DCP_FF}$) = 12·4 (see table 3) which approaches $\Delta\varepsilon$ ($1d_1$CP) = 15·2 (see table 1).

3.2. *Viscous and electro-optic properties*

From § 3.1 it follows that a broad range of material properties, especially dielectric anisotropies, can be achieved with the alkenyl liquid crystals shown in tables 1–3. However, the best set of material properties may be of little use if a single parameter which is crucial for the good overall performance of an electro-optic effect does not meet the performance standard of the set. Since the viscosity of a liquid crystal which essentially determines the dynamics of the display is such a crucial parameter, the viscous and visco elastic properties have to match these above good material properties.

The bulk viscosity η was determined with a rotating cone Brookfield micro-viscometer, whereas the rotational viscosity γ_1 was determined from the small angle relaxation of the nematic direction **n** caused by small pulsed magnetic fields. The static and dynamic electro-optic performance was investigated in transmissive twisted nematic displays. Collimated white light at vertical incidence and electrode gaps of 6 μm were used. The response times t_{on} and t_{off} correspond to the respective transmission changes 10 to 90 per cent and 100 to 10 per cent which result from applying the (temperature dependent) gated square wave driving voltage $V(T)$ = 2·5 × $V_{10}(T)$; where V_{10} is the optical threshold voltage at 10 per cent transmission. A summary of the measuring techniques is given in [4]. Comparisons of viscosities, viscoelastic ratios and twisted nematic response times should be made at constant temperatures, i.e. at 22°C in tables 7–9; whereas correlations between dielectric and elastic properties and threshold voltage should be made at the shifted temperatures (T_{NI} − 10°C).

Table 7 shows the bulk, η, and the rotational viscosity, γ_1, the viscoelastic ratio γ_1/κ and the dielectric anisotropy $\Delta\varepsilon$ of reference compound $3\mathrm{CPO}d_3 1$ and of the binary mixtures M1–M7 (see table 1). For positive dielectric anisotropic materials the threshold voltages V_{10} and the response times t_{on}, t_{off} are included. Because the determination of γ_1 requires a minimal anisotropic diamagnetic susceptibility $\Delta\chi \neq 0$ as well as a minimal dielectric anisotropy $\leqslant \varepsilon \neq 0$ [4], γ_1 and therefore also γ_1/κ could not be determined in all cases, cf. M3, M4 and M15. From M1–M5 in table 7 follows that the bulk and the rotational viscosities of all the new two ring alkenyls are considerably lower than those of the low viscosity reference $3\mathrm{CPO}d_3 1$. For γ_1 (M2), which comprises $1d_1$CC1O1, the reduction is 40 per cent. Because of the lower bulk viscosity of M3, the decrease of γ_1 is most likely still larger for $0d_1$CC5. As we have shown earlier the turn-off times t_{off} of twisted nematic displays depend not only on γ_1 but rather on the viscoelastic ratio, γ_1/κ [4, 5]. So far the lowest reported γ_1/κ values are those of binary mixtures comprising bicyclohexane alkenyl-alkoxy's where γ_1/κ

Table 8. Bulk (η) and rotational (γ_1) viscosities; viscoelastic ratio γ_1/κ; $\Delta\varepsilon$; V_{10}; t_{on} and t_{off} of mixtures M10–M14 comprising the para fluorinated alkenyls depicted in table 2. M8 and M9 comprise the alkyl-alkenyls of table 2. The data in bold type were determined at (T_{NI} − 10°C), whereas the others are 22°C data.

Liquid crystal	η/cP	γ_1/cP	$\gamma_1^{-1}\kappa/10^{-12}$ m^{-2} s^{-1}	$\Delta\varepsilon$	V_{10}/V	t_{on}/ms	t_{off}/ms
M8 = (**1*d*$_1$CCP1**, 3CPO*d*$_3$1)	**3·8**	**13·5**	**1·7**	**−0·110**	-	-	-
	13·8	94	3·7	−0·220			
M9 = (**0*d*$_3$CCP1**, 3CPO*d*$_3$1)	**3·8**	**9·3**	**1·3**	**−0·113**	-	-	-
	13·9	83	4·5	−0·220			
M10 = (**0*d*$_1$CCPF**, 3CPO*d*$_3$1)	**4·2**	**15·0**	**1·8**	**0·181**	**7·0**	**4·6**	**8·0**
	13·3	78	4·5	0·222	10·0	9·4	14
M11 = (**1*d*$_1$CCPF**, 3CPO*d*$_3$1)	**3·7**	**13·4**	**1·5**	**0·359**	**5·3**	**3·6**	**6·5**
	15·2	86	4·3	0·485	7·3	10	13
M12 = (**0*d*$_3$CCPF**, 3CPO*d*$_3$1)	**4·9**	**14·4**	**1·8**	**0·213**	**6·3**	**4·0**	**8·1**
	14·7	81	4·4	0·266	9·3	11	15
M13 = (**1*d*$_3$CCPF**, 3CPO*d*$_3$1)	**3·7**	**12·4**	**1·5**	**0·353**	**5·2**	**3·7**	**7·4**
	14·8	115	5·8	0·483	7·5	10	14
M14 = (**0*d*$_4$CCPF**, 3CPO*d*$_3$1)	**4·8**	**14·9**	**2·0**	**0·219**	**6·0**	**5·0**	**10·0**
	11·5	74	4·4	0·284	8·5	12	17

Table 9. Bulk (η) and rotational (γ_1) viscosities; viscoelastic ratio γ_1/κ; $\Delta\varepsilon$; V_{10}; t_{on} and t_{off} of mixtures M15–M19 comprise the para and laterally fluorinated 1d_1-alkenyls as well as fluorinated dioxane alkenyls. The data in bold type were determined at (T_{NI} − 10°C), whereas the others are 22°C data.

Liquid crystal	η/cP	γ_1/cP	$\gamma_1^{-1}\kappa/10^{-12}$ m^{-2} s^{-1}	$\Delta\varepsilon$	V_{10}/V	t_{on}/ms	t_{off}/ms
M8 = (**1d_1CCP1**, 3CPO$d_3$1)	**3·8**	**13·5**	**1·7**	**−0·110**	–	–	–
	13·8	94	4·7	−0·220			
M15 = (**1d_1CCP$_F$1**, 3CPO$d_3$1)	**4·3**	–	–	**−0·150**	–	–	–
	14·8			−0·262			
M11 = (**1d_1CCPF**, 3CPO$d_3$1)	**3·7**	**13·4**	**1·5**	**0·359**	**5·3**	**3·6**	**6·5**
	15·2	86	4·3	0·485	7·3	10	13
M16 = (**1d_1CCP$_F$F**, 3CPO$d_3$1)	**4·6**	**15·8**	**2·0**	**0·687**	**3·8**	**4·2**	**9·4**
	15·2	85	4·6	0·971	5·1	8·9	15
M17 = (**1d_1DCPF**, 3CPO$d_3$1)	**4·9**	**20·5**	**2·4**	**1·544**	**2·3**	**5·4**	**9·1**
	15·2	128	7·7	2·100	3·4	10	17
M18 = (**1d_1DCP$_F$F**, 3CPO$d_3$1)	**6·1**	**24·5**	**2·8**	**2·378**	**2·0**	**6·2**	**11**
	15·8	111	6·8	3·314	2·6	11	20
M19 = (**0d_1CCEPF**, 3CPO$d_3$1)	**4·2**	**12·5**	**1·5**	**0·202**	**6·5**	**4·0**	**8·3**
	15·2	105	5·7	0·230	10·2	10	18

(22°C) = $4{\cdot}0 \times 10^{-12}\,\mathrm{m^{-2}\,s^{-1}}$ [4]. From table 7 it follows that γ_1/κ of M2 and M3 are still lower and this in combination with favourably large mesomorphic ranges (see table 1). As expected from their dielectric anisotropies the para fluorinated compounds 0d_3CPF and 0d_3DPF exhibit markedly different threshold voltages V_{10} in mixtures M4 and M5 (see table 7). Their short response times t_{off}, which are comparable with those of the fastest cyano compounds used in M6 and M7, correspond with their low viscoelastic ratios and their low viscosities (see table 7).

Table 8 shows the viscous and the electro-optic properties of mixtures M8, M9 as well as those of M10–M14 which comprise the para fluorinated three ring alkenyls depicted in table 2. Comparing the viscosities of M8 with M11 and M9 with M12 shows that para fluorination leads to a slight viscosity reduction, this despite the increase of $\Delta\varepsilon$. Moreover, from the viscosities of 3CPO$d_3$1 in table 7 it follows that all three ring alkenyls in table 8, except 1d_3CCPF, do not exceed the viscosity of the low viscous two ring reference compound; this despite the increase of T_{NI} (M) by up to 21°C compared with T_{NI} (3CPO$d_3$1); cf. tables 1 and 2. For 0d_4CCPF (M14) even a γ_1 reduction of 14 per cent follows (see table 7). Therefore, and because of the rather large κ values (see table 5) low visco elastic ratios γ_1/κ (22°C) $\sim 4{\cdot}5$ result which lead to the short response times t_{off} of the new compounds in mixtures M10–M14 in table 7. As expected from their dielectric anisotropies the lowest threshold voltages result for 1d_1CCPF and 1d_3CCPF (cf. M11 and M13 in table 8).

Table 9 shows the viscous and the electro-optic properties of mixtures M15–M19 which comprise the para and laterally fluorinated 1d_1-alkenyls, as well as the fluorinated dioxane alkenyls (see table 3). From γ_1 (M11) $\approx \gamma_1$ (M16) $\approx \gamma_1$ (3CPO$d_3$1) = 86 cP it follows that the combination of para and lateral fluorination does not increase the rotational viscosity of 3CPO$d_3$1. This follows also from their identical, low bulk viscosities, their low viscoelastic ratios and from their comparably short turn-off times (see table 9). Moreover, this finding is confirmed by the similar viscosity data of M17 and M18 which comprise the dioxane alkenyls (see table 9). The increase of rotational viscosity in M17 and M18 is due to the replacement of a cyclohexane ring C by the dioxane ring D in the respective rigid cores. It is noteworthy that most viscoelastic ratios of the *three ring* compounds in table 9 are lower than those of the best *two ring* cyano compounds see table 7, [4, 5]. From table 9 it also follows that the introduction of an ester linkage in the rigid core leads to an increase of γ_1 which is not balanced by other favourable material properties.

The step-wise increase of $\Delta\varepsilon$ which results from the synergisms following from para + lateral fluorination and from replacing C by D is reflected in table 9 by the corresponding step-wise decrease of the threshold voltage V_{10}. Because of the proportionality between the optical threshold voltage V_{10} of twisted nematic displays and their threshold voltage V_{c} for mechanical deformation, if follows that [1]:

$$V_{10} \propto \pi\left(\frac{\kappa}{\varepsilon_0\Delta\varepsilon}\right)^{1/2}. \qquad (1)$$

From the elastic and dielectric data of M11 and M18 in table 6 and from equation (1) we obtain at (T_{NI} − 10°C) for the voltage ratio of the mixtures comprising 1d_1CCPF and 1d_1DCP$_{\mathrm{F}}$F:

$$\frac{V_{10}\,(\mathrm{M11})}{V_{10}\,(\mathrm{M18})} = \left(\frac{\kappa_{11}\Delta\varepsilon_{18}}{\Delta\varepsilon_{11}\kappa_{18}}\right)^{1/2} = 2{\cdot}59.$$

This ratio is in good agreement with the voltage ratio that follows from the threshold measurements given in table 9, i.e. from V_{10} (M11)/V_{10} (M18) = 2·65. Comparably, good agreement between the respective ratios which follows from the material parameters in table 6 and from those of V_{10} in table 9 result for V_{10} (M11)/V_{10} (M17) = 2·12 (2·30) and V_{10} (M11)/V_{10} (M16) = 1·39 (1·44).

4. Discussion

A number of new, low polar, two ring as well as three ring alkenyl liquid crystals with double bonds in selective side chain positions, different fluoro substituents and different rigid cores were designed so that wide nematic mesophases and a broad range of material properties resulted. Their dielectric, elastic, optic, viscous and electro-optic properties are shown to correlate with specific molecular structural elements. Synergisms follow from combining para and lateral fluorination of the benzene ring in the rigid cores and/or from selectively positioning the side chain double bonds and/or from replacing cyclohexane core rings by dioxane rings. From investigations of the dielectric properties, birefringence, viscosity viscoelasticity and the three elastic constants with the electro-optic performance in twisted nematic displays it follows that the new compounds favourably combine low viscosity, low viscoelastic ratios, high nematic–isotropic transition temperatures and a broad range of dielectric anisotropies. This renders them applicable in rapidly responding, high information content liquid crystal displays.

In agreement with our earlier results with bicyclohexane and phenylcyclohexane alkenyls [4, 5], we find pronounced odd–even effects by shifting the alkenyl double bond from even to odd side chain sites in the sterically comparable molecules $0d_4$CCPF and $1d_3$CCPF (see table 2). In the present work the effect is not so pronounced for the bend/splay elastic ratio k_{33}/k_{11} but it is most pronounced for the dielectric anisotropy $\Delta\varepsilon$ which increases by 40 per cent (see table 2). The mechanism which we proposed to explain the dielectric odd–even effect in alkenyls is based on our recent investigations of chain ordering by carbon-13 2D NMR spectroscopy [8]. From these investigations it follows that the chain order parameter in odd alkenyl double bond sites of the type $1d_{2n+1}$ is almost twice as large as the chain order of terminal double bonds at even sites, such as in the $0d_4$-alkenyls. Therefore, and because the π-electrons of the double bond contribute to the induced dipole moment parallel to the long molecular axis, we expect $\Delta\varepsilon$ as well as Δn to increase with increasing chain order. From the dielectric theory of nematic liquid crystals the dielectric anisotropy $\Delta\varepsilon$ [9] is given by

$$\Delta\varepsilon \propto \left[\Delta\alpha - F\frac{\mu^2}{2kT}(1 - 3\cos^2\beta)\right]S; \qquad (2)$$

with

$$S = \tfrac{1}{2}\langle 3\cos^2\theta - 1\rangle,$$

as the nematic order parameter; $\Delta\alpha = (\alpha_{\parallel} - \alpha_{\perp})$, is the anisotropy of induced molecular polarization; F is the Onsager internal electric field; μ, is the permanent molecular dipole moment; β is the angle between $\boldsymbol{\mu}$ and the molecular long axis. Equation (2) consists of an induced dipolar term $\Delta\alpha$ and of a permanent dipolar term $\boldsymbol{\mu}$ which are both affected by the nematic order parameter S. It follows from our previous discussion and equation (2) that $\Delta\varepsilon$ should indeed increase for odd double bonds in lower ordered even positions. Moreover, increased chain ordering or odd sites not only increase $\Delta\varepsilon$ but seems also to induce an increase of the nematic order parameter S. This follows from the strong increase of the nematic-isotropic transition temperatures in alkenyls with odd double bond sites (see table 2, [4, 5]). According to equation (2) both, increased chain ordering and increased nematic order lead to an increase of $\Delta\varepsilon$. Which of the two effects is dominant has yet to be investigated.

The results in table 5 confirm our previous findings [4, 5] on the double bond site dependent odd–even effects in alkenyls which affected $\Delta\varepsilon$, Δn, k_{33}/k_{11} and κ. They confirm moreover that the rotational viscosity γ_1 increases markedly when shifting double bonds from $0d_4$ (even) to $1d_3$ (odd) sites (cf. the 33 per cent increase between M13 and M14 in table 8 and also [4, 5]). This increase in γ_1 can also be related to the increase of the corresponding chain order, namely via the increased hindrance of reorientation of the long molecular axes in the nematic phase. If the origin of the rotational viscosity γ_1 is considered as the hindered reorientation of an ensemble of molecules which jumps by 180° between the two minima of the nematic mean field potential, then there must be a free volume, V, available for the ensemble to jump within a characteristic time $1/f$; where f is the dielectric relaxation frequency

$$\gamma_1 = \frac{kT}{\pi^2 V f}. \tag{3}$$

From computing V and f, Diogo and Martins derived [10]:

$$\gamma_1 \propto S^2 \exp\left[\frac{aS}{kT} + \frac{\theta S^2}{T - T_g}\right]; \tag{4}$$

where aS, is the height of the Maier–Saupe mean field potential [6]; and T_g, is the glass transition temperature. From equations (3) and (4) it follows that γ_1 decreases in nematics with increasing free volume, that is, with increasing side-chain disorder. Thus, if we assume that the increase of chain ordering from $S\,(0d_4) < S\,(1d_3)$ which we observed in all alkenyl classes investigated so far [8] also applies to the new alkenyls, then the observed viscosity increase γ_1 ($0d_4$CCPF) $<$ γ_1 ($1d_3$CCPF) qualitatively follows from equation (2).

We gratefully acknowledge the experimental assistance of B. Blöchliger, A. Germann, J. Reichardt and H. R. Saladin.

References

[1] SCHADT, M., 1989, *Liq. Crystals* **5**, 57; 1988, *Molec Crystals liq. Crystals*, **165**, 405.

[2] CHANDRASEKHAR, S., 1977, *Liquid Crystals* (Cambridge University Press).

[3] KANEKO, E., 1987, *Liquid Crystal TV Displays: Principles and Applications of Liquid Crystal Displays* (KTK Scientific Publishers).

[4] SCHADT, M., BUCHECKER, R., and MÜLLER, K., 1989, *Liq Crystals*, **5**, 293.

[5] SCHADT, M., BUCHECKER, R., LEENHOUTS, F., VILLIGER, A., and PETRZILKA, M., 1986, *Molec Crystals liq. Crystals*, **139**, 1; 1985, *Ibid.*, **122**, 241.

[6] MAIER, W., and SAUPE, A., 1959, *Z. Naturf.* (*a*), **14**, 882.

[7] BUCHECKER, R., and SCHADT, M., 1987, *Molec. Crystals liq. Crystals*, **149**, 359.

[8] FRECH, C. B., FUNG, B. M., and SCHADT, M., 1989, *SPIE*, **1080**, 215.

[9] MAIER, W., and MEIER, G., 1961, *Z. Naturf.* (*a*) **16**, 262.

[10] DIOGO, A. C., and MARTINS, A. F., 1981, *Molec. Crystals liq. Crystals*, **66**, 133.